*Available online at* www.derpharmachemica.com

ISSN 0975-413X
CODEN (USA): PCHHAX

**Der Pharma Chemica, 2017, 9(7):8-12**
*(http://www.derpharmachemica.com/archive.html)*

# Crystal Structure and Hirshfeld Surface Analysis of 4-Nitrophenyl Isocyanate

**Hema MK[1], Karthik CS[2,3], Karthik Kumara[1], Mallesha L[2], Mallu P[3], Lokanath NK[1*]**

[1]*Department of Studies in Physics, University of Mysore, Manasagangotri, Mysuru-570006, India*
[2]*Department of Chemistry, JSS College of Arts, Commerce and Science, Mysuru-570025, India*
[3]*Department of Chemistry, Sri Jayachamarajendra College of Engineering, Mysuru-570006, India*

## ABSTRACT

*The compound, 4-nitrophenyl isocyanate ($C_7H_4N_2O_3$) was crystallized from dichloromethane and the single crystal was studied by X-ray diffraction studies. The title compound is crystallized in the monoclinic crystal system with the space group $P2_1/n$. The unit cell parameters are a=3.7123(11) Å, b=13.120(3) Å, c=15.041(4) Å, β=93.648(15)° and V=731.1(3)Å$^3$. The structure exhibits inter-molecular hydrogen bonds of the type C—H...O, which accounts for the stability of the molecule. The intermolecular interactions in the crystal structure were quantified and analyzed using Hirshfeld surface analysis.*

**Keywords:** Isocyanates, Hirshfeld surface, X-ray diffraction, Direct method

## INTRODUCTION

Isocyanates play a significant role in the pharmaceutical industry and also in many other industrial fields related to special and fine chemistry. The discovery of polyurethanes by Bayer triggered the interest in isocyanates and eventually resulted in the application of mono and di-isocyanates in a variety of polymers, plastics, adhesives and coatings [1-3]. Aromatic isocyanates like phenyl isocyanate and 3,4-dichlorophenyl isocyanate are intermediates in speciality chemicals as well, their carbamate derivatives intervene in the synthesis of various pesticides like Metolcarb, Carbofuran, Pirimicarb, Isoprocarb and Diethofencarb. In the polymer field, polyisocyanates such as 2,4-toluene di-isocyanate and methylene 4,4'-diphenyl di-isocyanate are starting materials for the synthesis of many polyurethanes [4,5]. Isocyanates used as an electrolyte additive in lithium ion batteries because of its anion receptors to improve electrochemical and chemical stability [6]. Isocyanate group may slow down solid electrolyte interphase decomposition in lithium ion batteries by functioning as radical trapper [7].

In pharmaceutical industry, aromatic isocyanates represent very important intermediates that can be converted into different functionalities such as carbamates, semicarbazides and urea [8]. Many drugs containing carbamates and urea moiety has been synthesized by different isocyanates. Carbamates can be considered as 1:1 adducts of isocyanates and alcohols and urea yields the related isocyanate and amine. Carbamates and urea are intermediates for the preparation of pesticides and fertilizers [9]. Among them, urea represents an extensively used tremendous class of compounds with multi-focal applications in several fields such as fertilizers, drug synthesis, therapeutic agents, etc. [10]. Methyl N-(triethylammoniumsulfonyl) carbamate is synthesized from chlorosulfonyl isocyanate (known as Burgess Reagent), a dehydrating agent, which is used in various synthetic transformations and in the synthesis of various heterocyclic systems [11]. Attributed to the above facts, we report herein crystallization of 4-nitrophenyl isocyanate and the structure was confirmed by X-ray diffraction studies.Further, Hirshfeld surface analysis including $d_{norm}$ surfaces and 2D Fingerprint plots were performed and the results of the analysis are discussed.

## MATERIALS AND METHODS

### Crystallization of 4-nitro phenyl isocyanate

All solvents and reagents were purchased from Sigma Aldrich Chemicals Pvt. Ltd. and Merck. Synthesis and other characterization are reported earlier [12]. 4-nitro phenyl isocyanate (Figure 1) is dissolved in dichloromethane as solvent. The mixture is warmed and kept for slow evaporation, which yields yellow coloured crystals.

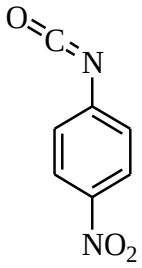


**Figure 1: Schematic diagram of 4-nitro phenyl isocyanate**

## RESULTS AND DISCUSSION

### Single crystal X-ray diffraction method

A yellow colored rectangle shaped single crystal of dimension 0.25 × 0.30 × 0.35 mm of the title compound was selected for data collection. X-ray intensity data were collected for the title compound at temperature 293 K on a Rigaku XtaLABmini CCD diffractometer with X-ray generator operating at 45 kV and 10 mA, using $MoK_{\alpha}$ radiation of wavelength 0.71073 Å. X-ray intensity data were collected, keeping the scan width of 0.5°, exposure time of 3 s, the sample to detector distance of 50 mm. A complete data set was processed using Crystal Clear [13]. The structure was solved by direct methods and refined by full-matrix least squares method on $F^2$ using SHELXS and SHELXL programs, respectively [14]. All the non-hydrogen atoms were revealed in the first difference Fourier map itself. The geometrical calculations were carried out using Platon [15] and the packing diagrams were generated using Mercury [16].

X-ray diffraction analysis revealed that the title compound is crystallized in the monoclinic crystal system with the space group $P2_1/n$. The unit cell parameters are a=3.7123(11) Å, b=13.120(3) Å, c=15.041(4) Å, β=93.648(15)° and V=731.1(3)Å$^3$. The ORTEP view of the title molecule with displacement ellipsoids drawn at 50% probability level is shown in Figure 2. The packing of molecules when viewed down *a*-axis is as given in Figure 3. The crystal data and structure refinement details are given in Table 1. A total of 110 parameters were refined with 1662 unique reflections, which converged the residual to R=0.0621. The bond lengths and bond angles values are within the expected range, which are given in Table 2. Torsion angles are given in Table 3 and hydrogen-bond geometry is given in Table 4.

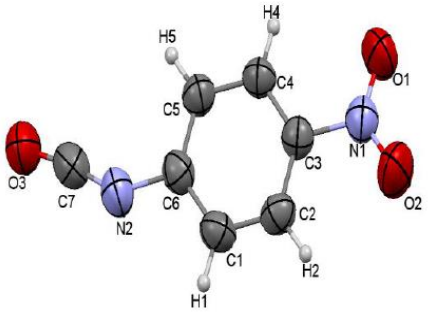


**Figure 2: ORTEP diagram of the molecule with thermal ellipsoids drawn at 50% probability**

The C3–N1 bond connecting the nitro group is the longest bond length with 1.459(3) Å. The O–N bonds (O1–N1: 1.212(3) Å; O2–N1: 1.209(3) Å) shows double bond (1.20 Å) [17] and the O1–N1–O2 angle is 122.68(19)°, which is common for aromatic nitro groups. And the angle of O3-C7-N2 is 171.9(3)°. The phenyl ring of all carbon atoms are $sp^2$ hybridized, which are confirmed by their average bond angle value of 120°.

The phenyl ring is highly planar, and nitrogen of both isocyanate and nitro group attached to phenyl ring is planar. They are well described by torsion angles of C2-C1-C6-N2 (−179.70(19)°);C1-C2-C3-N1(−179.91(18)); N1-C3-C4-C5 (−179.70(17)) and C4-C5-C6-N2 (−179.93(19)), and they show anti-periplanar conformation. The structure exhibits inter-molecular hydrogen bonds of the type C—H...O. The inter molecular hydrogen bond C(2)-H(2)...O(2) has a length of 3.3575 Å and an angle of 149° with symmetry code *1-x, 1-y, -z*. Another inter molecular hydrogen bond C(5)-H(5)...O(1) has a length of 3.3459 Å and an angle of 151° with symmetry code *5/2-x,-1/2+y,1/2-z*.

**Table 1: Crystal data and structure refinement details**

| Parameter | Value |
|---|---|
| CCDC deposit No. | 1469530 |
| Empirical formula | $C_7H_4N_2O_3$ |
| Formula weight | 164.12 |
| Temperature | 293 *K* |
| Wavelength | 0.71073 Å |
| Crystal system, space group | Monoclinic, *P* $2_1/n$ |
| Unit cell dimensions | *a*=3.7123(11) Å<br>*b*=13.120(3) Å<br>*c*=15.041(4) Å<br>α=90°<br>β=93.648(15)°<br>γ=90° |

| | |
|---|---|
| Volume | 731.1(3)Å$^3$ |
| *Z* | 4 |
| Density (calculated) | 1.491 Mg m$^{-3}$ |
| Absorption coefficient | 0.120 mm$^{-1}$ |
| $F_{000}$ | 336 |
| Crystal size | 0.25 × 0.30 × 0.35 mm |
| θ range for data collection | 3.11-27.62° |
| Index ranges | $-4 \le h \le 4$<br>$-15 \le k \le 17$<br>$-15 \le l \le 19$ |
| Reflections collected | 3150 |
| Independent reflections | 1662 [$R_{int}$=0.0381] |
| Absorption correction | Multi-scan |
| Refinement method | Full matrix least-squares on $F^2$ |
| Data/restraints/parameters | 1662/0/110 |
| Goodness-of-fit on $F^2$ | 1.068 |
| Final [$I > 2\sigma(I)$] | $R1$=0.0621, $wR2$=0.1766 |
| R indices (all data) | $R1$=0.0851, $wR2$=0.2108 |
| Extinction coefficient | 0.01(2) |
| Largest diff. peak and hole | 0.245 and −0.200 e Å$^{-3}$ |

**Table 2: Selected bond lengths and angles (Å, ◦ )**

| | | | |
|---|---|---|---|
| O1-N1 | 1.212(3) | O2-N1-C3 | 119.12(19) |
| O2-N1 | 1.209(3) | C6-N2-C7 | 140.1(2) |
| O3-C7 | 1.160(3) | N1-C3-C2 | 118.40(17) |
| N1-C3 | 1.459(3) | N1-C3-C4 | 118.97(17) |
| N2-C6 | 1.395(3) | N2-C6-C1 | 117.78(19) |
| N2-C7 | 1.181(3) | N2-C6-C5 | 121.19(19) |
| O1-N1-O2 | 122.68(19) | O3-C7-N2 | 171.9(3) |
| O1-N1-C3 | 118.20(17) | C1-C6-C5 | 121.0(2) |

**Table 3: Selected Torsion angles (°)**

| | | | |
|---|---|---|---|
| O1-N1-C3-C4 | −5.6(3) | C7-N2-C6-C1 | −170.6(3) |
| O2-N1-C3-C4 | 174.2(2) | C2-C1-C6-N2 | −179.70(19) |
| O1-N1-C3-C2 | 174.29(19) | C1-C2-C3-N1 | −179.91(18) |
| O2-N1-C3-C2 | −5.9(3) | N1-C3-C4-C5 | −179.70(17) |
| C7-N2-C6-C5 | 10.3(5) | C4-C5-C6-N2 | −179.93(19) |

**Table 4: Hydrogen-bond geometry (Å, ◦)**

| D—H...A | D—H | H...A | D...A | D—H...A | Symmetry code |
|---|---|---|---|---|---|
| C(2)-H(2)...O(2) | 0.93 | 2.53 | 3.3575 | 149 | 1-x, 1-y, -z |
| C(5)-H(5)...O(1) | O.93 | 2.5 | 3.3459 | 151 | 5/2-x,-1/2+y,1/2-z |

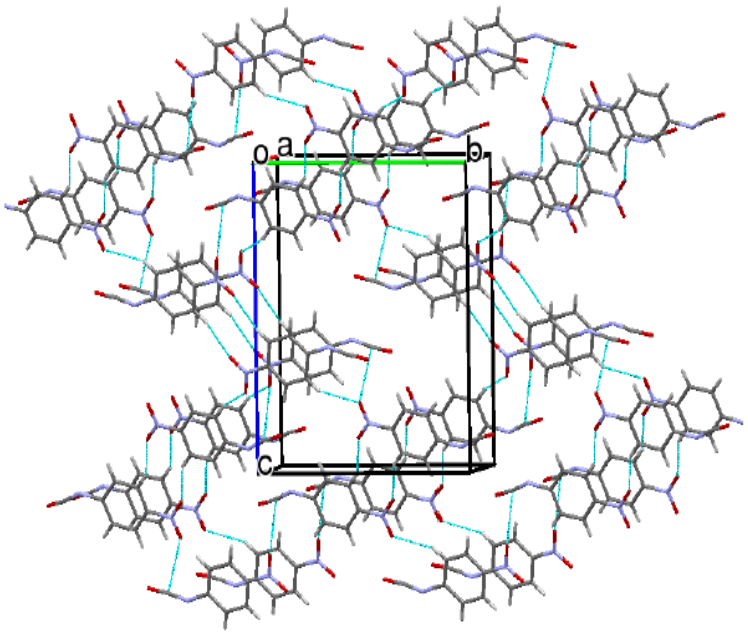


**Figure 3: Molecular packing view of the title compound down the *a*-axis**

**Hirshfeld surface analysis**

The 3D Hirshfeld surfaces and 2D fingerprint plots are unique for any crystal structure. They serve as powerful tools for gaining additional insight into crystal structure. The 2D fingerprint plots can give a quantitative summarization of the nature and type of intermolecular contacts experienced by the molecules in the crystal and at the same time, it can also be broken down to give the relative contribution to the Hirshfeld surface area from each type of interactions present, quoted as the "contact contribution". Fingerprint plots of the title compound are shown in Figure 4.

The H…O/O…H intermolecular interactions appear as distinct spikes in the 2D fingerprint plot; the most significant contribution to the total Hirshfeld surfaces (50.5%). Complementary regions are visible in the fingerprint plots where one molecule acts as a donor and the other as an acceptor. The H…O interaction are represented by a spike ($d_i$=1.1 Å, $d_e$=1.38 Å) in the bottom left (donor) area, whereas the O…H interactions are represented by a spike ($d_i$=1.38 Å, $d_e$=1.1 Å) in the bottom right region in the fingerprint plot. The minor contribution is from H…C (10.3%) and C…N (5.9%) to total Hirshfeld surface area of the molecule. These contacts are highlighted by a conventional mapping of $d_{norm}$ on the molecular Hirshfeld surface (Figure 5). The red colored regions on the $d_{norm}$ surface represent the intermolecular contacts closer than the sum of the van der Waals radii; the blue region shows the longer contacts. Intermolecular interaction of the crystal structure shown in Figure 6.

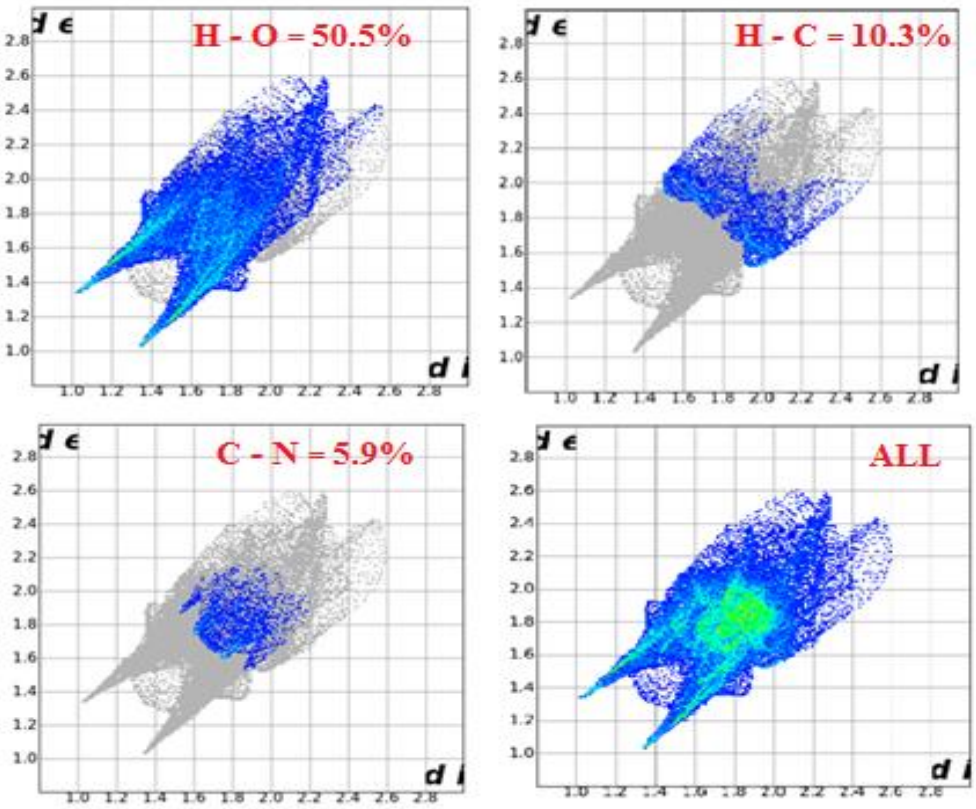


**Figure 4: Fingerprint plots of the title compound showing H...O, H...C and C...N interactions. $d_i$ is the closest internal distance from a given point on the Hirshfeld surface and $d_e$ is the closest external contacts**

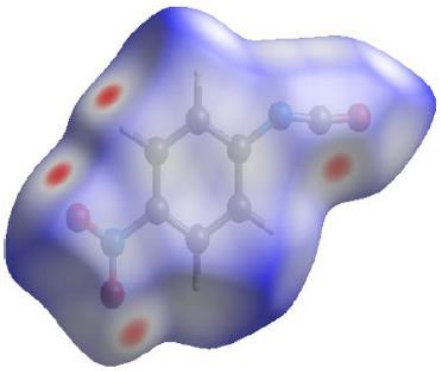

**Figure 5: The Hirshfeld surface of crystal mapped with $d_{norm}$, the red spots indicate donor-acceptor interactions**

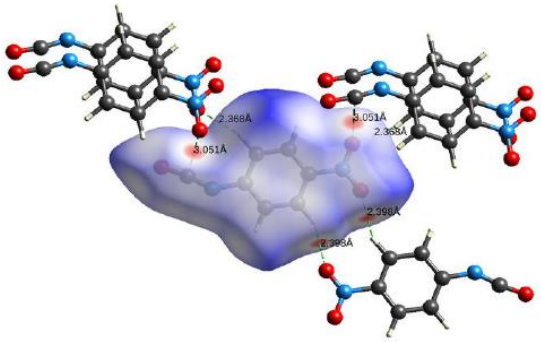


**Figure 6: Intermolecular interaction of the crystal structure**

## CONCLUSION

The present work helps us to understand the molecular structure and the intermolecular interactions of the title compound. The structure was confirmed by X-ray diffraction. The structure exhibits inter molecular hydrogen bonds of the type C—H...O. Molecular Hirshfeld surfaces revealed that the compound was supported mainly by O...H intermolecular interactions. The fingerprint plots identified the types of intermolecular interactions present in the crystal.

## ACKNOWLEDGMENTS

MKH is thankful to DST- PURSE, Vijnana Bhavan, University of Mysore, Mysuru for financial assistance. Authors would like to thank National single crystal X-ray diffractometer facility laboratory, DoS in Physics, University of Mysore, Mysuru.

## REFERENCES

[1] M.A. Gauthier, M.I. Gibson, H.A. Klok, *Angewand. Chemie. Int. Ed*., **2009**, 48(1), 48.
[2] D. Bello, J. Sparer, C.A. Redlich, K. Ibrahim, M.H. Stowe, Y. Liu, *J. Occup. Environ. Hyg.*, **2007**, 4(6), 406.
[3] N.S. Allen, M. Edge, A. Ortega, C.M. Liauw, J. Stratton, R.B. McIntyre, *Polym. Degrad. Stab*., **2002**, 78(3), 467.
[4] A.S. More, T. Lebarbe, L. Maisonneuve, B. Gadenne, C. Alfos, H. Cramail, *Eur. Poly. J*., **2013**, 49(4), 823-833.
[5] I. Javni, W. Zhang, Z.S. Petrovic, *J. App. Poly. Sci.*, **2003**, 88(13), 2912.
[6] C. Korepp, W. Kern, E.A. Lanzer, P.R. Raimann, J.O. Besenhard, M.H. Yang, M. Winter, *J. Power. Sour*., **2007**, 174(2), 387.
[7] F. Wu, J. Xiang, L. Li, J. Chen, G. Tan, R. Chen, *J. Power. Sour*., **2012**, 202, 322.
[8] A.K. Ghosh, M. Brindisi, *J. Med. Chem*., **2015**, 58(7), 2895.
[9] F. Paul, *Chem. Rev*., **2000**, 203(1), 269.
[10] S. Mustafa, S. Perveen, A. Khan, *J. Serb. Chem. Soc*., **2014**, 79(1), 1.
[11] S. Khapli, S. Dey, D. Mal, *J. Indian. Inst. Sci*., **2013**, 81(4), 461.
[12] J.S. Potts, A.A. Sayigh, U. Henri, (Upjohn Company), U.S. Patent 3,341,564, **1967**.
[13] Rigaku, *Cryst. Clear*., **2011**.
[14] G.M. Sheldrick, *Acta. Cryst*., **2015**, 71, 3.
[15] A.L. Spek, *Acta. Cryst*., **1990**, 46, 34.
[16] C.F. Macrae, I.J. Bruno, J.A. Chisholm, P.R. Edgington, P. McCabe, E. Pidcock, L. Rodriguez-Monge, R. Taylor, J. van de Streek, P.A. Wood, *J. Appl. Cryst*., **2008**, 41, 466.
[17] M. Klapotke, D.T. Izsak, *Crystals.*, **2012**, 2(2), 294.